SLAC–PUB–7304
February 1997

Longitudinal space charge in final-focus systems for linear colliders*

Frank Zimmermann and Tor O. Raubenheimer
Stanford Linear Accelerator Center
Stanford University, Stanford, CA 94309, USA

In the final-focus system of a linear collider, the effect of longitudinal space charge can be significant. A diverging or converging ultra-relativistic beam experiences a longitudinal space-charge force which is independent of the beam energy. This force, though weak and often neglected, causes an energy variation across the bunch which depends on the beam size, beam-pipe radius and bunch population and this may affect the chromatic correction of a beam line. Because of the inherent large chromaticity of a typical final-focus system, a very small energy variation, induced in the final focus, can lead to an intolerable increase of the spot size at the interaction point. The space-charge force, thus, gives rise to a limit on bunch intensity beyond which the resulting spot-size increase will degrade the collider performance. In this paper, we evaluate the effect of the longitudinal space charge and derive intensity limits for three existing or proposed final foci.

Submitted to Nuclear Instruments and Methods in Physics Research A

*Work supported by Department of Energy contract DE–AC03–76SF00515.

1 INTRODUCTION

The purpose of a final-focus system for a linear collider is to demagnify a high-energy electron (or positron) beam to a minuscule vertical spot size at the interaction point (IP). The last focusing before the IP is achieved with two or three strong quadrupoles, a so-called final doublet or triplet. At these quadrupoles the values of the beta functions are huge, up to tens or hundreds of kilometers, and, as a result, the system is highly chromatic.

The chromaticity is conventionally canceled by upstream sextupole magnets at locations with nonzero dispersion, *i.e.*, where there is a correlation between a particle's transverse displacement and its energy deviation. In order to achieve the desired small spot sizes at the IP, the chromaticity needs to be compensated very accurately for all particles in a bunch. But, small changes to the particle energy distribution which occur between the sextupoles and the final quadrupoles will impair this chromatic correction and may lead to an increase of the IP spot size.

The chromatic contribution to the vertical spot size at the IP can be written

$$\frac{\Delta\sigma_y}{\sigma_y} = \xi_y \, (\Delta\delta)_{rms}, \tag{1}$$

where the dimensionless number ξ_y characterizes the vertical chromaticity of the final doublet, and $(\Delta\delta)_{rms}$ denotes the rms difference of the particle-energies at sextupoles and final quadrupoles, divided by the average beam energy E_b. The term $\Delta\sigma_y$ of Eq. (1) has to be added in quadrature to the design spot size.

As an example, $\xi_y \approx 6000$ in the final focus of the Stanford Linear Collider (SLC) at the Stanford Linear Accelerator Center (SLAC) [1], $\xi_y \approx 26,000$ for the Final Focus Test Beam (FFTB) at SLAC [2], and $\xi_y \approx 32,000$ for the Next Linear Collider (NLC) design [3]. Thus, the rms energy difference $(\Delta\delta)_{rms}$ between sextupoles and final quadrupoles at which the total spot size increases by 2% is about 3×10^{-5}, 8×10^{-6}, and 6×10^{-6}, for SLC, FFTB and NLC, respectively.

These are very small numbers—orders of magnitude smaller than the incoming beam energy spread. They reflect the sensitivity of the spot size to intra-bunch energy variations which occur in the final focus itself. A harmful energy variation $(\Delta\delta)_{rms}$ can be caused by forces so small that they would usually be ignored, in view of the high beam energy.

In this paper, we consider one such potentially harmful force, the longitudinal space-charge. Usually, when considering ultra-relativistic beams, the space-charge fields are neglected. This is done because, for particles in straight line motion, the normally considered longitudinal force scales inversely with the square of the relativistic Lorentz factor γ, which for high-energy linear colliders varies between 10^5 and 10^6, making the force negligible. In this paper, we calculate another source of longitudinal space-charge force which arises when the particles in the beam converge or diverge, as illustrated in Fig. 1. This force does not depend upon γ and thus can be important in the final-focus beam line since it causes the beam energy and energy spread to vary with location. The force can be simply understood from energy conservation arguments: when the beam size is decreased, the potential energy due to the mutual repulsion of the electrons or positrons in the beam is increased; this energy must come from the kinetic energy of the beam.

We note that the energy of the particles in a bunch will also be modified by the longitudinal wakefields which arise from the electromagnetic interaction between the beam and its surroundings, *i.e.*, the vacuum chamber. This additional energy variation may either counteract or enhance the space-charge effect and is not included in our analysis. An estimate of the wakefield effects in the NLC final-focus system can be found in Ref. [4], although, since the vacuum system has not yet been designed, this estimate is only a rough approximation. Reference [4] showed that, for a proper vacuum-chamber design, the wakefield effects in the final focus should not be a problem.

In the next sections, we will calculate the longitudinal space-charge force

and derive simple formulae to estimate its importance. The results are then applied to the SLC, FFTB, and NLC final-focus systems. Finally, we compare these estimates with simulation results from a particle tracking code which includes the longitudinal space-charge force.

2 LONGITUDINAL SPACE-CHARGE FORCE

The longitudinal space-charge force causes both an energy shift and an energy variation along the bunch, which depend on beam size, beam-pipe radius, and bunch population. As discussed, the space-charge induced energy variation changes with location and thus may affect the chromatic correction. Because it is intensity-dependent, a limit on the bunch intensity exists beyond which the resulting spot-size increase will degrade the final-focus performance. An estimate of the critical intensity is obtained by comparing typical values for the space-charge induced relative energy spread $(\Delta\delta)_{rms}$ with the maximum tolerable value given in Section 1.

To this end, let us consider an ultra-relativistic electron (or positron) bunch traversing at the center of a perfectly conducting circular beam pipe which is assumed to be at zero potential. It is convenient to introduce a 'beam rest system', by which we mean the inertial reference frame moving along the (sufficiently straight) beam line at a velocity equal to the time-averaged velocity of the bunch centroid. In the such-defined rest frame, and for typical parameters, the instantaneous velocity of the bunch centroid is non-relativistic, and thus, in this system, magnetic fields generated by the beam can be neglected. Henceforth, the primed quantities will refer to the beam rest frame and the unprimed quantities to the laboratory system.

Suppose now that the bunch passes the location $s = 0$ at time $t = 0$, and also suppose that the transverse beam distribution is Gaussian. Consider a particle, *i.e.*, an electron or a positron, on the beam axis (x,y=0) at a longitudinal

distance

$$z \equiv s - vt \tag{2}$$

from the bunch center. Here, $v \approx c$ denotes the velocity of the bunch centroid. In the beam rest frame, the electrostatic potential energy $e\Phi'(x', y', z', s')$ of this particle is given by

$$e\Phi'(0, 0, z', s') = \frac{e\lambda'(z')}{4\pi\epsilon_0}\left(C + \ln 2 - 2\ln\left(\frac{\sigma_x(s') + \sigma_y(s')}{R(s')}\right)\right), \tag{3}$$

where $C \approx 0.577\ldots$ denotes Euler's constant, e the electron charge, $R(s)$ is the beam-pipe radius, $\sigma_x(s')$ and $\sigma_y(s')$ are the horizontal and vertical rms beam sizes, respectively, and λ' is the charge line density at longitudinal position z' within the bunch.

The line density in the laboratory frame is simply $\lambda(z) = \lambda'(z')\gamma$. Since the electric potential transforms as $\Phi = \gamma\Phi'$, Eq. (3) is also valid in the laboratory frame when one replaces the rest-frame line density λ' by the corresponding line density λ for the laboratory frame and the potential Φ' by Φ. Thus, in the laboratory system the electric potential at location s and position z within the bunch is

$$e\Phi(0, 0, z, s) = \frac{e\lambda(z)}{4\pi\epsilon_0}\left(C + \ln 2 - 2\ln\left(\frac{\sigma_x(s) + \sigma_y(s)}{R(s)}\right)\right). \tag{4}$$

Next, the longitudinal component of the magnetic vector potential in the laboratory frame reads

$$A_s(x, y, z, s) = \beta\gamma\Phi'(x, y, z', s') = \beta\Phi(x, y, z, s) \tag{5}$$

where β is the particle velocity. Considering the position s and time t as the independent variables, the corresponding potentials are $\tilde{\Phi}(x, y, s, t) \equiv \Phi(x, y, s - vt, s)$, $\tilde{A}_s(x, y, s, t) \equiv A_s(x, y, s - vt, s)$ (remember that $z \equiv s - vt$). Now, it is easy to see that the longitudinal electric field in the laboratory frame can be expressed in terms of the derivatives of the electric potential $\Phi(x, y, z, s)$ alone:

$$\mathcal{E}_s = -\frac{\partial\tilde{\Phi}}{\partial s} - \frac{1}{c}\frac{\partial\tilde{A}_s}{\partial t} = -\frac{\partial\Phi}{\partial s} - \frac{\partial\Phi}{\partial z}\frac{1}{\gamma^2}. \tag{6}$$

The last term describes the normally considered component of the space-charge force which arises from the non-uniformity of the longitudinal distribution and is very important at lower energies. From now on, we will neglect this term since it is suppressed by $1/\gamma^2$. For an ultra-relativistic beam the prevailing part of the longitudinal space-charge force is due to the dependence of the potential Φ on the location s, *i.e.*, due to changes in the transverse beam size or the beam-pipe radius which are encountered as the beam travels along the beam line. In this case, to a very good precision, the longitudinal space-charge force can be approximated by

$$\mathcal{E}_s \approx -\frac{\partial \Phi}{\partial s}, \tag{7}$$

where, as before, Φ denotes the electric potential in the laboratory frame as given in Eq. (4). Equation (7) states that, for an ultra-relativistic particle, the change of the longitudinal kinetic energy due to the space-charge force approximately equals the change in its potential energy $e\Phi$.

According to Eqs. (4) and (7), the kinetic (or potential) energy of an on-axis particle at a distance z from the bunch center changes between two locations by the amount

$$E_2(z) - E_1(z) = \frac{e\lambda(z)}{2\pi\epsilon_0} \ln\left(\frac{(\sigma_x+\sigma_y)_2 R_1}{(\sigma_x+\sigma_y)_1 R_2}\right), \tag{8}$$

where the subindices 1 and 2 refer to the two different locations. Since a change of the average bunch energy is easily corrected by adjusting the magnet strengths, it is the spread of energy change, *i.e.*, the rms change across the bunch, which is harmful.

For simplicity, we will henceforth assume that not only the transverse, but also the longitudinal distribution is Gaussian, *i.e.*, that the line density is given by

$$\lambda(z) = \frac{Ne}{\sqrt{2\pi}\sigma_z} e^{-\frac{z^2}{2\sigma_z^2}}, \tag{9}$$

where N denotes the number of particles per bunch. In this case, both the average

and the rms energy change can be estimated from the z-dependence of $\Phi(0,0,z,s)$ in Eq. (4),

$$(\Delta\delta)_{rms} \approx 0.28 \times \frac{2Nr_e}{\sqrt{2\pi}\sigma_z\gamma} \ln\left(\frac{\sigma_{sum,2}R_1}{\sigma_{sum,\ 1}R_2}\right), \tag{10}$$

where $\sigma_{sum} \equiv (\sigma_x + \sigma_y)$ denotes the sum of the two transverse rms sizes, r_e the classical electron radius, and the coefficients are calculated by performing the appropriate integrals over the beam distribution and the force. The average energy change $(\Delta\delta)_{ave}$ is about a factor 2.5 larger than the rms change $(\Delta\delta)_{rms}$.

Note that, in Eq. (10), we have ignored the dependence of the potential on the transverse position. This yields an estimate of the effect but is insufficient for more detailed calculations. To include the transverse variation of the longitudinal force, we can express the electric potential of a Gaussian charge distribution, with transverse rms sizes σ_x and σ_y, as [6]

$$\Phi(x,y,z) = \frac{\lambda(z)}{4\pi\epsilon_0}\int_0^\infty \frac{e^{-\frac{x^2}{2\sigma_x^2+q}+\frac{y^2}{2\sigma_y^2+q}}}{\sqrt{2\sigma_x^2+q}\sqrt{2\sigma_y^2+q}}dq, \tag{11}$$

provided that the longitudinal charge density $\lambda(z)$ is a sufficiently smooth function, *i.e.*,

$$\frac{1}{\lambda}\frac{d\lambda(z)}{dz} \ll \frac{\gamma}{\sigma_{x,y}}, \tag{12}$$

which is generally the case. Assuming σ_x and σ_y are slowly varying with location s, the potential $\Phi(x,y,z,s)$ also depends on s and satisfies the differential equation

$$\frac{\partial\Phi}{\partial s} \approx \frac{d\sigma_x^2}{ds}\frac{\partial\Phi}{\partial\sigma_x^2} + \frac{d\sigma_y^2}{ds}\frac{\partial\Phi}{\partial\sigma_y^2}. \tag{13}$$

This can be re-expressed as

$$\frac{\partial\Phi}{\partial s} \approx \frac{1}{2}\frac{d\sigma_x^2}{ds}\frac{\partial^2\Phi}{\partial x^2} + \frac{1}{2}\frac{d\sigma_y^2}{ds}\frac{\partial^2\Phi}{\partial y^2} \tag{14}$$

by noting that $\partial\Phi/\partial\sigma_{x,y}^2 = \frac{1}{2}\partial\Phi^2/\partial(x,y)^2$. Of course, in order for Eq. (14) to be valid, the variation of $\sigma_{x,y}$ with position s needs to be small so that

$$\frac{d\sigma_x}{ds}, \frac{d\sigma_y}{ds} \ll \gamma, \tag{15}$$

which is easily fulfilled in all the examples considered.

According to Eq. (7), the derivative of the electric potential, $-\partial\Phi/\partial s$, approximately equals the longitudinal space-charge field $\mathcal{E}_s$. Equation (14) shows that the force $e\mathcal{E}_s$ experienced by a particle of charge e can be expressed in terms of the derivative of the transverse forces $F_{x,y}$ as follows:

$$e\mathcal{E}_s \approx \frac{1}{2}\frac{d\sigma_x^2}{ds}\frac{\partial F_x}{\partial x} + \frac{1}{2}\frac{d\sigma_y^2}{ds}\frac{\partial F_y}{\partial y} = \left[-\alpha_x\epsilon_x + \eta_x\eta_x'\sigma_\delta^2\right]\frac{\partial F_x}{\partial x} - \alpha_y\epsilon_y\frac{\partial F_y}{\partial y}. \qquad (16)$$

Here, $\epsilon_{x,y}$ are the horizontal and vertical beam emittances and the parameters $\alpha_{x,y}$ describe the convergence of the beam: the $\langle xx'\rangle$ and $\langle yy'\rangle$ second moments of the beam distribution are equal to $-\alpha_x\epsilon_x$ and $-\alpha_y\epsilon_y$. Finally, σ_δ is the rms relative energy spread and η_x is the horizontal dispersion, *i.e.*, the momentum dependence of the horizontal position, and $\eta_x' = d\eta_x/ds$; note that we have assumed that the vertical dispersion is zero which is usually the case in linear collider final-focus systems.

For illustration, a typical longitudinal space-charge field for a beam in the NLC final focus is plotted as a function of the horizontal (a) and vertical (b) position, in Fig. 2. Notice that the variation in the vertical plane is somewhat smaller than that in the horizontal plane, and that the field reverses sign at large horizontal amplitudes. The difference between the two planes arises because the beam is flat with an aspect ratio $\sigma_x/\sigma_y \gg 1$.

3 ESTIMATES

Given the optics of a final focus, we can use Eqs. (1) and (10) to estimate the effect of the space-charge force in this system. Specifically, we want to compare the difference in energy between the chromatic correction sextupoles and the final lenses. Furthermore, because the colliders operate with flat beams, the vertical plane is much more sensitive to energy variation than the horizontal.

In the SLC final focus, we have $\sigma_{sum} \approx 850$ μm at the Y-sextupoles and

$\sigma_{sum} \approx 1.71$ mm inside Q2, the center magnet of the final triplet. Next, in the FFTB, the beam size at the Y-sextupoles $\sigma_{sum} \approx 650$ μm almost equals that at the center of the final quadrupole $\sigma_{sum} \approx 570$ μm. Finally, for the 500-GeV center-of-mass energy NLC design, the beam sizes are $\sigma_{sum} \approx 337$ μm at the Y-sextupoles and $\sigma_{sum} \approx 250$ μm inside the first quadrupole Q1. In all three examples, the beam-pipe radii in the sextupoles and in the final quadrupoles are about the same.

Assuming typical operating or design currents (4×10^{10}, 1×10^{10} and 0.65×10^{10} particles per bunch) and bunch lengths of 700 μm, 600 μm, and 100 μm, the rms energy difference $(\Delta\delta)_{rms}$ induced between sextupoles and final quadrupoles is 2.5×10^{-7}, 1.4×10^{-8}, and 2.5×10^{-8}, for SLC, FFTB and NLC, respectively, and, using Eq. (1), the critical current for a 2% spot size increase is estimated to be more than an order of magnitude larger than the present design or operating current. This is a crude estimate, since the beam sizes inside the final quadrupoles change rapidly, the chromaticity of other final-focus magnets has been neglected, and, in Eq. (10), we have ignored the dependence of the potential on the transverse coordinates.

We can also estimate the change of the beam energy at the IP. In the SLC, the IP beam size is 2 μm $\times$ 500 nm. The NLC is designed for a spot size of 300 nm $\times$ 4.5 nm. These numbers imply a change of the average beam energy at the IP, relative to that inside the last quadrupoles, by -280 keV in the SLC and -350 keV for the NLC, which is more than hundred times smaller than the rms energy spread of the beam and, thus, most likely insignificant.

4 SIMULATION STUDIES

To study the space-charge induced spot-size increase and the IP energy change in more detail, *e.g.*, to include the dependence of the space-charge force on transverse position, and to compare the results with the above estimates, we have modified

the multi-particle tracking code MAD [5] by adding the energy variation due to the space charge. In the simulation, the space-charge force is calculated solely from the change of the transverse beam dimensions, since, for the systems considered, the beam-pipe aperture variation is small in comparison.

Since compact expressions for the transverse field of a Gaussian charge distribution are readily available—for example see Ref. [7]—it is straightforward, under the above assumptions, to include the longitudinal space-charge force in a six-dimensional tracking program such as MAD. In our simulation, a multi-particle distribution (typically 10,000 particles) is propagated step by step through the magnets and drift spaces of the final-focus system. After each step, of length Δs, the relative energy deviation δ of a particle with coordinates x, y and z is changed by an amount $\Delta\delta$ according to Eq. (16), which, for a flat beam ($\sigma_x \gg \sigma_y$), reads

$$\begin{aligned}\Delta\delta(x,y,z) &= -\Delta s \cdot \frac{\lambda(z) r_e}{\gamma}\left(\frac{2\pi}{\sigma_x^2-\sigma_y^2}\right)^{\frac{1}{2}}\Big[\alpha_y\epsilon_y\frac{\partial}{\partial y}\ \text{Re}\ \mathcal{F}(x,y)+ \\ &\quad +(\alpha_x\epsilon_x-\eta_x\eta_x'\sigma_\delta^2)\frac{\partial}{\partial x}\ \text{Im}\ \mathcal{F}(x,y)\Big] \qquad (17)\end{aligned}$$

where σ_x and σ_y denote the rms beam sizes at location s, and $\mathcal{F}(x,y)$ is defined in terms of the complex error function W as

$$\mathcal{F}(x,y) = W\left(\frac{x+iy}{(2(\sigma_x^2-\sigma_y^2))^{\frac{1}{2}}}\right) - e^{-\frac{x^2}{2\sigma_x^2}-\frac{y^2}{2\sigma_y^2}} W\left(\frac{\frac{\sigma_y}{\sigma_x}x+i\frac{\sigma_x}{\sigma_y}y}{(2(\sigma_x^2-\sigma_y^2))^{\frac{1}{2}}}\right). \qquad (18)$$

The function $\mathcal{F}$ is familiar from the Bassetti-Erskine representation for the transverse fields of a Gaussian charge distribution [7], and the derivatives $\partial F/\partial y$ and $\partial F/\partial x$ are easily obtained. For a tall beam ($\sigma_y \gg \sigma_x$) the coordinates x and y need to be interchanged. The step size Δs in Eq. (17) has to be chosen small enough that the rms sizes $\sigma_{x,y}$ do not change appreciably over this distance:

$$\Delta s \ll \frac{\sigma_x}{d\sigma_x/ds}, \frac{\sigma_y}{d\sigma_y/ds}. \qquad (19)$$

If the beam is round ($\sigma_x = \sigma_y$), Eq. (17) becomes singular. Therefore, for a nearly round beam ($\sigma_x \approx \sigma_y$) we approximate the relative energy deviation by the

round-beam formula

$$\Delta\delta(x,y,z) \approx -\Delta s \cdot \frac{2\lambda(z) r_e}{\gamma}\left[\alpha_y\epsilon_y \frac{\partial}{\partial y}\,\frac{f_{r,y}(x,y)}{\partial y} + (\alpha_x\epsilon_x - \eta_x\eta_x'\sigma_\delta^2)\frac{\partial f_{r,x}}{\partial x}\right], \quad (20)$$

where we have used the abbreviations $r^2 \equiv x^2 + y^2$, $\sigma \equiv \sqrt{\sigma_x\sigma_y} \approx \sigma_x \approx \sigma_y$,

$$f_{r,x} \equiv \frac{x}{r^2}\left(1 - e^{-\frac{r^2}{2\sigma^2}}\right) \quad (21)$$

and

$$f_{r,y} \equiv \frac{y}{r^2}\left(1 - e^{-\frac{r^2}{2\sigma^2}}\right). \quad (22)$$

It is notable that at small amplitudes ($x/\sigma_x \ll 1$, $y/\sigma_y \ll 1$) the energy change for both flat and round beams, Eqs. (17) and (20), simplifies to

$$\Delta\delta(z) \approx -\frac{\Delta s\; 2\lambda(z) r_e}{\gamma(\sigma_x + \sigma_y)}\left[\frac{\alpha_y\epsilon_y}{\sigma_y} + \frac{\alpha_x\epsilon_x - \eta_x\eta_x'\sigma_\delta^2}{\sigma_x}\right], \quad (23)$$

which is independent of the transverse position.

In our simulation, the space-charge force is calculated according to the aforementioned equations, including the dependence of the field on the transverse position and assuming that at each location the beam is of Gaussian shape with the design transverse rms size. If the space-charge force (or any other effect diluting the emittance) is so large that the beam distribution either deviates strongly from a Gaussian or spreads out in the transverse phase space, a more self-consistent treatment would be warranted. For the applications considered in this paper, however, the space-charge force is weak enough that the simple treatment described above appears adequate.

Typical tracking results including space charge are presented in Figs. 3–5. Figures 3 and 4 display the variation of the average bunch energy along the NLC and SLC final foci, respectively. The magnitude of the energy variation is consistent with our earlier estimates. It seems fortuitous that, in both systems, the energy difference between sextupoles and the last quadrupoles is much smaller than the 'typical' energy variation. This arises, in part, because the beams are

large in the sextupoles where η_x is large to ease the sextupole strengths and the beams are large in the final lenses before focusing them to tiny spots at the IP.

As a further example, Fig. 5 depicts the energy variation in an odd-dispersion final focus, designed by Oide [8], for roughly the same IP beam parameters as in Fig. 3. In this system only the second Y-sextupole is used for chromatic correction. This particular odd-dispersion design is slightly more sensitive to space-charge than the design of Fig. 3, although the effect is still small.

Table 1 lists the spot-size increases obtained by multi-particle tracking. The spot sizes change sensibly for bunch populations larger than a few times 10^{11} particles. As expected from Eqs. (1) and (10), the relative spot-size increase (to be added in quadrature) is proportional to the beam intensity. In the simulation, no attempt was made to correct for the change of average beam energy. Thus, assuming that the magnet strengths will be adapted to the actual local beam energy, the real intensity limit will be about two times higher than that predicted by Table 1.

5 CONCLUSION

In this paper, we have discussed a component of the longitudinal space-charge force that is not usually considered. In the final focus system of a linear collider, this force could place a limit on the achievable luminosity. For the NLC, FFTB and SLC final foci, the longitudinal space-charge force was found to be significant only for bunch populations an order of magnitude larger than their design or operating value. For a different final-focus optics the critical intensity could be considerably lower and, therefore, the space-charge effect deserves attention during the design phase. In addition to the spot-size increase, the longitudinal space-charge force also causes a change of the average beam energy at the IP, which, although rather small, might prove important in the analysis of high-precision experiments.

As a final point, it should be noted that we have only considered effects of

the longitudinal space-charge force that occur in the final focus of linear colliders. Similar effects will arise in other beam lines which are sensitive to the cancelation of chromatic effects such as bunch compressors. In addition, we should note that we have only evaluated the longitudinal force caused by variations in the beam size. The longitudinal space-charge force can also be significant in bending magnets [9], although, for the parameters we considered here, this effect is not important. We also have not considered the effect of the longitudinal wakefields in the beam line nor have we considered the wakefield-like effect of coherent synchrotron radiation [10, 11] in the bending magnets. The former effect is straightforward to calculate and imposes some simple limitations on the vacuum chamber design [4], while the latter effect is still a subject of active research and needs further investigation.

ACKNOWLEDGMENTS

This work was supported by Department of Energy Contract No. DE-AC03-76SF00515.

References

[1] The SLC (Stanford Linear Collider) at the Stanford Linear Accelerator Center (SLAC) is the first and only linear collider in operation. A discussion of its recent performance and parameters by P. Emma can be found in the *Proceedings of the 1995 IEEE Particle Accelerator Conference* (IEEE, Piscataway, 1996), p. 606.

[2] The Final-Focus Test Beam (FFTB) built by an international collaboration at SLAC is a prototype final-focus system for a future linear collider. Recent results with measured design spot sizes have been described by Alexandrof et al., *Proceedings of the 1995 IEEE Particle Accelerator Conference* (IEEE, Piscataway, 1996), p. 2742.

[3] The NLC (Next Linear Collider) is a future linear collider being designed at the Stanford Linear Accelerator Center (SLAC). Parameters for its final-focus system can be found in the *Zeroth Order Design Report for the Next Linear Collider*, SLAC Report 474, 1996 (unpublished).

[4] T.O. Raubenheimer and F. Zimmermann, "Longitudinal Wake Fields and Chromatic Spot-Size Dilution in the NLC Final Focus," (SLAC) NLC–Note–23 (1996) (unpublished).

[5] H. Grote and F. C. Iselin, "The MAD Program, Version 8.1, User's Reference Manual", CERN Report No. CERN/SL/90–13, 1990 (unpublished).

[6] S. Kheifets, "Potential of a three-dimensional Gaussian bunch", DESY Report PETRA Note 119, 1976 (unpublished).

[7] M. Bassetti, G. A. Erskine, "Closed Expression for the Electric Field of a Two-Dimensional Gaussian Charge", CERN Report CERN–ISR–TH/80–06, 1980 (unpublished).

[8] K. Oide, "Final Focus System with Odd Dispersion Scheme", *Proceedings of the XVth International Conference on High Energy Accelerators HEACC 92*, International Journal of Modern Physics A, p. 861, 1993.

[9] B.E. Carlsten and T.O. Raubenheimer, "Emittance Growth of Bunched Beams in Bends," *Phys. Rev. E* **51:** 1453 (1995).

[10] R.L. Warnock, "Shielded Coherent Synchrotron Radiation and its Effect on Very Short Bunches," Proc. of the 4th Advanced ICFA Beam Dynamics Workshop on Collective Effects in Short Bunches, Tsukuba, Japan (1990) p. 151.

[11] Y.S. Derbenev, J. Rossbach, E.L. Saldin, V.D. Shiltsev, "Microbunch Radiative Tail-Head Interaction," (DESY) TESLA–FEL 95–05 (1995) (unpublished).

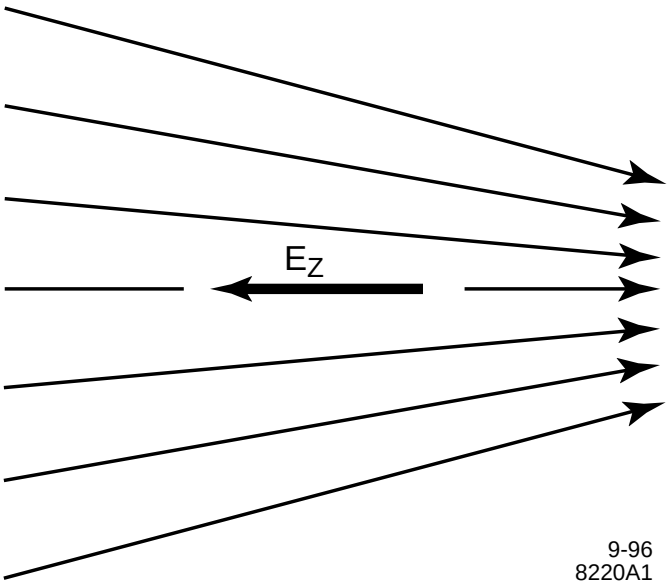

Figure 1: Longitudinal field in converging beam.

N	$\Delta\sigma_y/\sigma_{y0}$			
	SLC	FFTB	NLC	odd-η NLC
1×10^{11}	5.1%	0.3%	8.4 %	15.7%
2×10^{11}	9.8%	0.6%	24.6 %	30.9%
4×10^{11}	17.4%	1.3%	55.5 %	61.2%

Table 1: Simulated relative increase of the vertical spot size due to longitudinal space-charge, for different numbers of particles per bunch N. The design spot sizes σ_{y0} are 370 nm, 44 nm and 4.5 nm, for SLC, FFTB and NLC, respectively, to which the contribution $\Delta\sigma_y$ has to be added in quadrature.

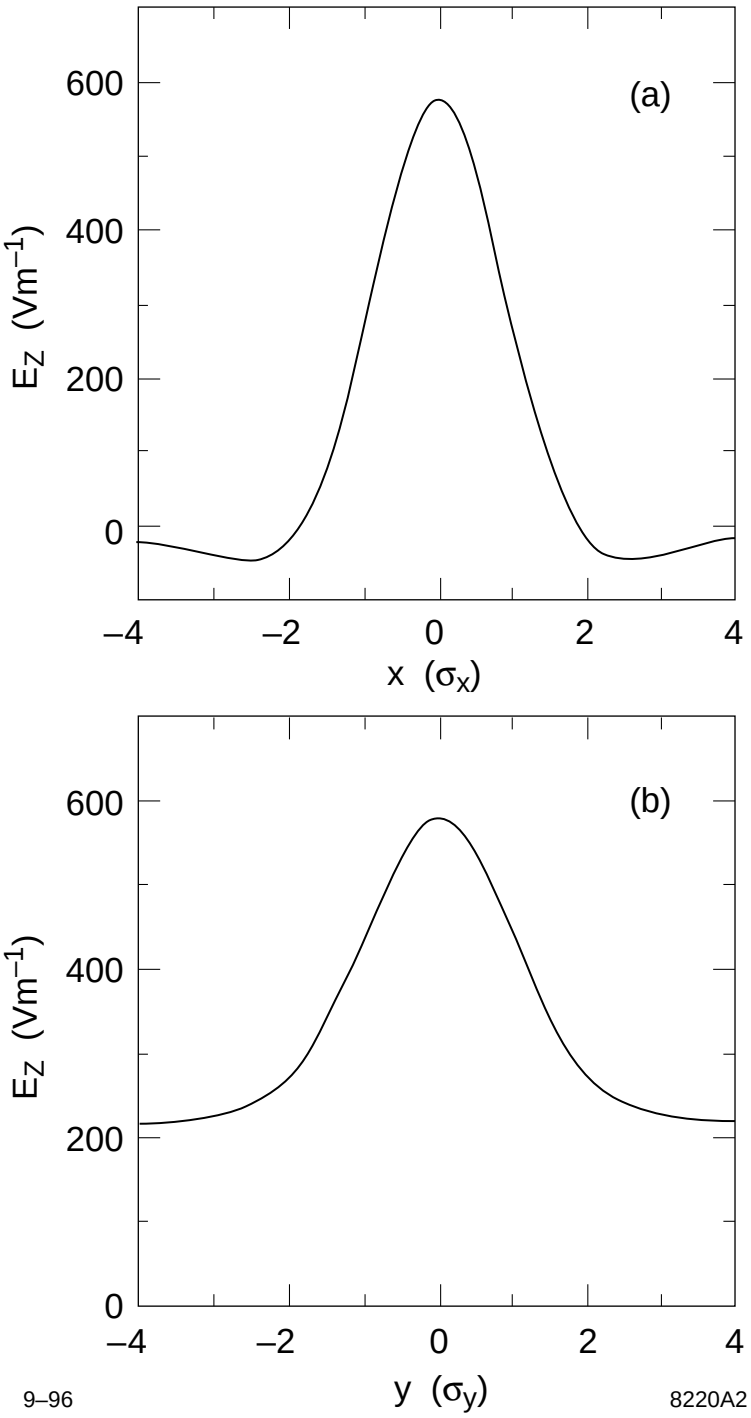

Figure 2: Longitudinal field versus horizontal (a) and vertical (b) position in a converging positron beam at a typical location in the NLC final focus. The beam energy is 250 GeV and normalized emittances are $\gamma\epsilon_x = 5$ mm-mrad and $\gamma\epsilon_y = 0.09$ mm-mrad while $\alpha_x = 0.3$ and $\alpha_y = 0.5$. The beam sizes are $\sigma_x = 30\mu$m, $\sigma_y = 0.65\mu$m, and $\sigma_z = 100\mu$m, and the number of particles per bunch is 0.65×10^{10}.

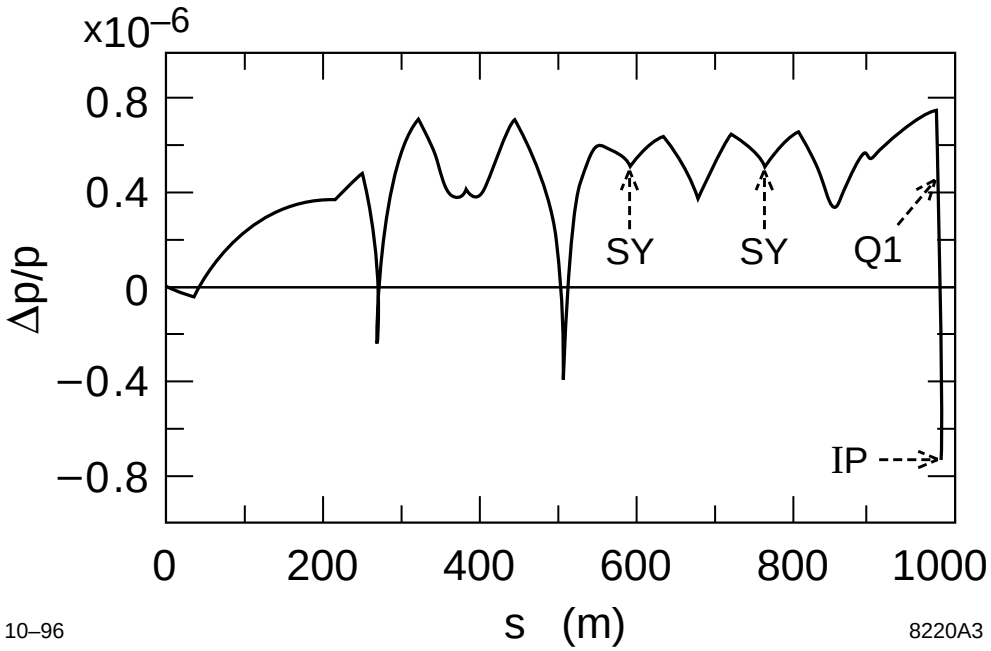

Figure 3: Variation of average bunch energy due to the longitudinal space-charge force in a 500 GeV center-of-mass energy NLC final focus system, for a bunch length of 100 μm and 6.5×10^9 particles per bunch; the locations of the vertical sextupoles and the final quadrupole are noted.

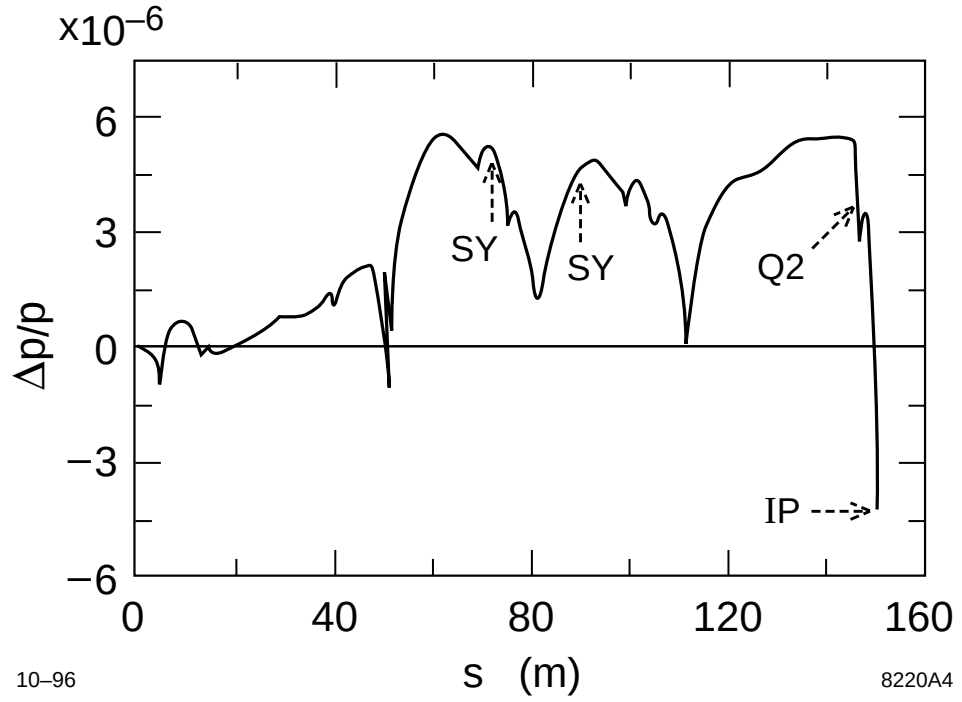

Figure 4: Variation of average bunch energy due to longitudinal space-charge force in the SLC final focus system, for a bunch length of 700 μm and 4×10^{10} particles per bunch; the locations of the vertical sextupoles and the final vertically focusing quadrupole are noted.

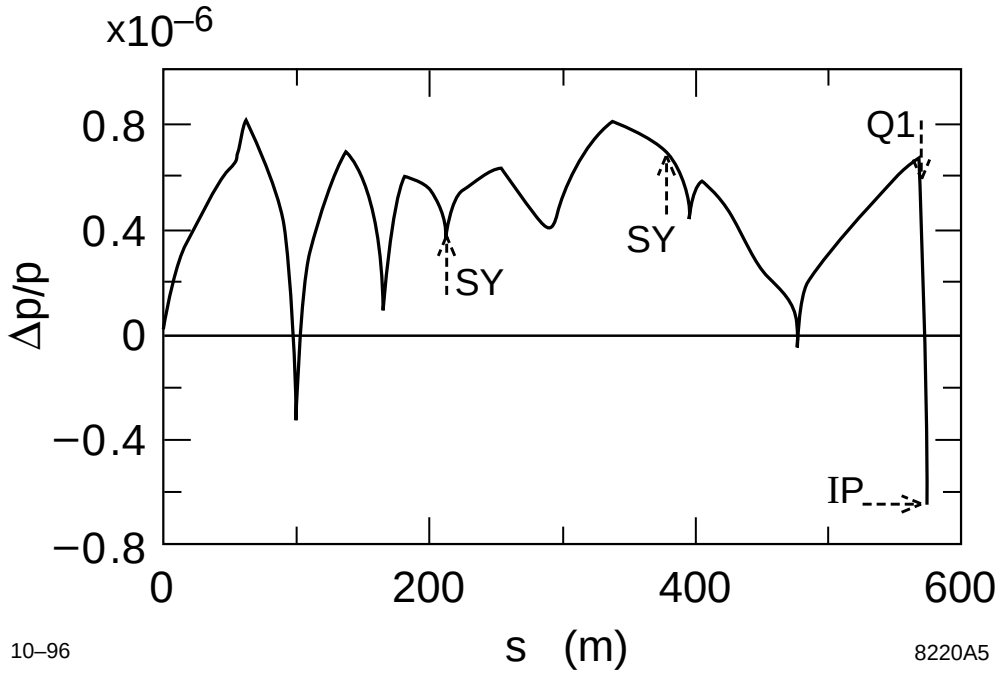

Figure 5: Variation of average bunch energy due to longitudinal space-charge force in a 500-GeV center-of-mass energy odd-dispersion final focus system; beam parameters are the same as for Fig. 3; the locations of the vertical sextupoles and the final quadrupole are noted.